Plasticity Tool for Predicting Shear Nonlinearity of Unidirectional Laminates under Multiaxial Loading

John T. Wang and Geoffrey F. Bomarito

ABSTRACT

This study implements a plasticity tool to predict the nonlinear shear behavior of unidirectional composite laminates under multiaxial loadings, with an intent to further develop the tool for use in composite progressive damage analysis. The steps for developing the plasticity tool include establishing a general quadratic yield function, deriving the incremental elasto-plastic stress-strain relations using the yield function with associated flow rule, and integrating the elasto-plastic stress-strain relations with a modified Euler method and a substepping scheme. Micromechanics analyses are performed to obtain normal and shear stress-strain curves that are used in determining the plasticity parameters of the yield function. By analyzing a micromechanics model, a virtual testing approach is used to replace costly experimental tests for obtaining stress-strain responses of composites under various loadings. The predicted elastic moduli and Poisson's ratios are in good agreement with experimental data. The substepping scheme for integrating the elasto-plastic stress-strain relations is suitable for working with displacement-based finite element codes. An illustration problem is solved to show that the plasticity tool can predict the nonlinear shear behavior for a unidirectional laminate subjected to multiaxial loadings.

INTRODUCTION

Unidirectional laminates contain very stiff fibers and a compliant matrix, and they behave nonlinearly when the matrix is significantly loaded, such as under transverse and shear loadings. Plasticity models have been found to be useful for predicting the nonlinear behavior [1-6]. The one-parameter plasticity model developed by Sun et al. [1] is particularly appealing, because of its simplicity and accuracy in predicting the nonlinear stress-strain relationships for two dimensional (2D) plane stress problems. Three dimensional (3D) plasticity models for composites have also been developed. Xie and Adams [2] developed a 3D orthotropic plasticity model for modeling

Durability, Damage Tolerance & Reliability Branch, Research and Technology Directorate, NASA Langley Research Center, Hampton, VA 23681, USA

unidirectional composite materials. Chen et al. [3] developed a quadratic yield function for fiber-reinforced composites which relaxes two commonly used assumptions: that hydrostatic stresses do not influence the plastic deformation, and the total plastic dilatation is incompressible. Recently, Goldberg et al. [5-6] developed an orthotropic plasticity model in which both plasticity and damage can be incorporated.

Shear nonlinearities can have significant effects on composite structural responses and strengths [7-13]. For example, Wang et al. [7] found that shear nonlinearity can reduce buckling loads by 57% for composite cylindrical shells. The shear nonlinearities need to be properly modeled for accurate structural loading responses and strength predictions. Many researchers have attempted to include shear nonlinearity in analytical models in order to obtain more accurate strength predictions [8-13]. However, most commercial codes for progressive damage analysis (PDA) assume linear shear stress-strain relations.

The objective of this study is to implement a plasticity tool for predicting the nonlinear shear behavior of unidirectional composite laminates under multiaxial loadings. The steps for developing the plasticity tool include establishing a general quadratic yield function [3, 14], deriving the incremental elasto-plastic stress-strain relations using the yield function with an associated flow rule [15-16], and integrating the elasto-plastic stress-strain relations for predicting the shear nonlinearity of unidirectional laminates under multiaxial loads [17-19]. To establish the general quadratic yield function [3], stress-strain curves of unidirectional laminates under various loading conditions are needed. In this study, a micro-mechanics based 3D representative volume element (RVE) is developed and analyzed with various loading conditions [20] to generate these stress-strain curves. The stress-strain curves obtained by the RVE analyses are used to determine the plasticity parameters of the yield function [3, 5-6]. A substepping scheme [17-19], based on the well-known modified Euler method, is used in this study for integrating the elasto-plastic stress-strain relations. The substepping scheme is suitable for use with finite element plasticity calculations that solve for the stress increments, assuming the strain increments are known. The implemented scheme is applicable to any general type of constitutive law and can control the error in the integration process by adjusting the size of each substep automatically [19]. At the end of the paper, an illustration problem is solved to show that the plasticity tool can predict the nonlinear shear behavior for a unidirectional laminate subjected to multiaxial loadings.

PLASTICITY TOOL

A plasticity tool for predicting the nonlinear behavior of a unidirectional laminate under multiaxial loading is presented. The plasticity tool uses a generalized, quadratic, orthotropic yield function proposed by Chen et al. [3]. The associated flow rule [15, 16] is used to derive the incremental elasto-plastic stress-strain relations. A micro-mechanics based 3D representative volume element (RVE) is developed and analyzed with various loading conditions [20] to generate the stress-strain curves of a unidirectional laminate under various loading conditions. These stress-strain curves

are then used for determining the plasticity parameters of the yield function [3, 5-6]. Finally, the incremental elasto-plastic stress-strain relations are integrated to predict the nonlinear behavior of unidirectional laminates under multiaxial loading.

Yield Function and Elasto-plastic Stress-strain Relations

A generalized, quadratic, orthotropic yield function proposed by Chen et al. [3] is used in this study,

$$\begin{aligned} f(\sigma_{ij}) = {} & a_{11}\sigma_{11}^2 + a_{22}\sigma_{22}^2 + a_{33}\sigma_{33}^2 + 2a_{12}\sigma_{11}\sigma_{22} + 2a_{23}\sigma_{22}\sigma_{33} \\ & + 2a_{13}\sigma_{11}\sigma_{33} + 2a_{44}\sigma_{23}^2 + 2a_{55}\sigma_{31}^2 + 2a_{66}\sigma_{12}^2 = k \end{aligned} \tag{1}$$

where the stresses σ_{ij} refer to the principal material directions [21], and k is a state variable representing the hardening parameter. The yield function contains nine plasticity parameters a_{ij}, which describe the amount of anisotropy in the plasticity. The nine plasticity parameters are assumed to be constants.

The yield function (Eq. 1) can be reduced to Hill's orthotropic yield function [14] when

$$\begin{aligned} a_{12} &= a_{33} - (a_{11} + a_{22} + a_{33})/2 \\ a_{13} &= a_{22} - (a_{11} + a_{22} + a_{33})/2 \\ a_{23} &= a_{11} - (a_{11} + a_{22} + a_{33})/2 \,. \end{aligned} \tag{2}$$

Using the associated flow rule [15-16], the incremental plastic strains $d\varepsilon_{ij}^p$ can be written as

$$d\varepsilon_{ij}^p = d\lambda \frac{\partial f}{\partial \sigma_{ij}}, \tag{3}$$

in which p denotes plasticity, and $d\lambda$ is a scalar plastic multiplier. Equation 3 can be explicitly expressed as

$$\begin{Bmatrix} d\varepsilon_{11}^p \\ d\varepsilon_{22}^p \\ d\varepsilon_{33}^p \\ d\gamma_{23}^p \\ d\gamma_{31}^p \\ d\gamma_{12}^p \end{Bmatrix} = \begin{Bmatrix} a_{11}\sigma_{11} + a_{12}\sigma_{22} + a_{13}\sigma_{33} \\ a_{12}\sigma_{11} + a_{22}\sigma_{22} + a_{23}\sigma_{33} \\ a_{13}\sigma_{11} + a_{23}\sigma_{22} + a_{33}\sigma_{33} \\ 2a_{44}\sigma_{23} \\ 2a_{55}\sigma_{31} \\ 2a_{66}\sigma_{12} \end{Bmatrix} (2d\lambda) \,. \tag{4}$$

Note that $d\gamma_{ij}^p$ denotes engineering shear strains and $d\varepsilon_{ij}^p$ denotes tensorial shear strains. Define plastic Poisson's ratios (PPRs) as

$$\nu_{ij}^{p} = -\frac{d\varepsilon_{jj}^{p}}{d\varepsilon_{ii}^{p}} \quad \text{(no summation over } i \text{ and } j\text{)} \tag{5}$$

for unidirectional loading in the i-direction. If all a_{ij} in Eq. 1 are constants, the following relationships can be obtained

$$\begin{aligned} &a_{11} = a_{22}\frac{\nu_{21}^{p}}{\nu_{12}^{p}}, \quad a_{33} = a_{22}\frac{\nu_{23}^{p}}{\nu_{32}^{p}}, \quad a_{11} = a_{33}\frac{\nu_{31}^{p}}{\nu_{13}^{p}}, \\ &a_{12} = -a_{22}\nu_{21}^{p}, \quad a_{23} = -a_{22}\nu_{23}^{p}, \quad a_{13} = -a_{33}\nu_{31}^{p}. \end{aligned} \tag{6}$$

The values of a_{44}, a_{55}, and a_{66}, are defined based on the effective stress and effective plastic strain curve that is established for the unidirectional laminate as follows:

Let the effective stress be defined as

$$\bar{\sigma} = \sqrt{\frac{3}{2} f} \ . \tag{7}$$

From Eqs. 1 and 7, the hardening parameter is

$$k = \frac{2}{3}\bar{\sigma}^{2} \ . \tag{8}$$

Using the concept of plastic work [14], the stresses and the incremental plastic strains can be related to the effective stress and the incremental effective plastic strain

$$dW^{p} = \sigma_{ij} d\varepsilon_{ij}^{p} = \bar{\sigma} d\bar{\varepsilon}^{p} \ . \tag{9}$$

Note that the increment of plastic work is per unit volume. From Eqs. 1, 4, and 9, the incremental effective plastic strain can be expressed as

$$d\bar{\varepsilon}^{p} = \frac{4}{3}\bar{\sigma} d\lambda \ . \tag{10}$$

Multiplying Eq. 10 by $d\bar{\varepsilon}^{p}$ and using Eqs. 1 and 9, one can obtain

$$(d\bar{\varepsilon}^{p})^{2} = \frac{8}{3} f (d\lambda)^{2} \ . \tag{11}$$

Substituting Eq. 1 into Eq. 11 and with the inversion of Eq. 4 for σ_{ij}, Eq. 11 can be explicitly expressed as

$$(d\bar{\varepsilon}^p)^2 = \frac{2}{3\Delta}[A_{11}(d\varepsilon_{11}^p)^2 + A_{22}(d\varepsilon_{22}^p)^2 + A_{33}(d\varepsilon_{33}^p)^2 + 2A_{12}d\varepsilon_{11}^p d\varepsilon_{22}^p + 2A_{23}d\varepsilon_{22}^p d\varepsilon_{33}^p + 2A_{13}d\varepsilon_{11}^p d\varepsilon_{33}^p] + \frac{4}{3}[\frac{(d\varepsilon_{23}^p)^2}{a_{44}} + \frac{(d\varepsilon_{31}^p)^2}{a_{55}} + \frac{(d\varepsilon_{12}^p)^2}{a_{66}}] \quad (12)$$

where

$$\Delta = \begin{vmatrix} a_{11} & a_{12} & a_{13} \\ a_{12} & a_{22} & a_{23} \\ a_{13} & a_{23} & a_{33} \end{vmatrix} \quad (13)$$

and

$$A_{11} = a_{22}a_{33} - a_{23}^2,\ A_{22} = a_{11}a_{33} - a_{13}^2,\ A_{33} = a_{11}a_{22} - a_{12}^2,$$
$$A_{12} = a_{13}a_{23} - a_{12}a_{33},\ A_{13} = a_{12}a_{23} - a_{13}a_{22},\ A_{23} = a_{12}a_{13} - a_{11}a_{23}. \quad (14)$$

Using Ref. 3, the $\bar{\sigma}$ *vs* $\bar{\varepsilon}^p$ relationship for each of the three normal and shear loadings can be obtained from Eqs. 1, 7, and 12. For normal loading σ_{ii}, the effective stress is

$$\bar{\sigma} = \sqrt{\frac{3a_{ii}}{2}}\sigma_{ii} \quad (i = 1, 2, \text{or } 3) \quad (15)$$

and the incremental effective plastic strain is

$$d\bar{\varepsilon}^p = \sqrt{\frac{2}{3a_{ii}}}d\varepsilon_{ii}^p \quad (i = 1, 2 \text{ or } 3). \quad (16)$$

For shear loading σ_{ij}, the effective stress is

$$\bar{\sigma} = \sqrt{3a_{rr}}\sigma_{ij} \quad (17)$$

where $rr = 44, 55, \text{or } 66,$ depending upon the shear stress components.
The incremental effective plastic strain for the shear loading is

$$d\bar{\varepsilon}^p = 2d\varepsilon_{ij}^p / \sqrt{3a_{rr}}. \quad (18)$$

For isotropic hardening, the yield surface is convex and the plastic strain increment is normal to the yield surface; the effective strain grows whenever the material is actively yielding and the effective plastic stress increases. If the unidirectional composite is undergoing isotropic hardening, a master $\bar{\sigma}$ *vs* $\bar{\varepsilon}^p$ curve can be established from any of the three normal and shear stress-strain curves. The

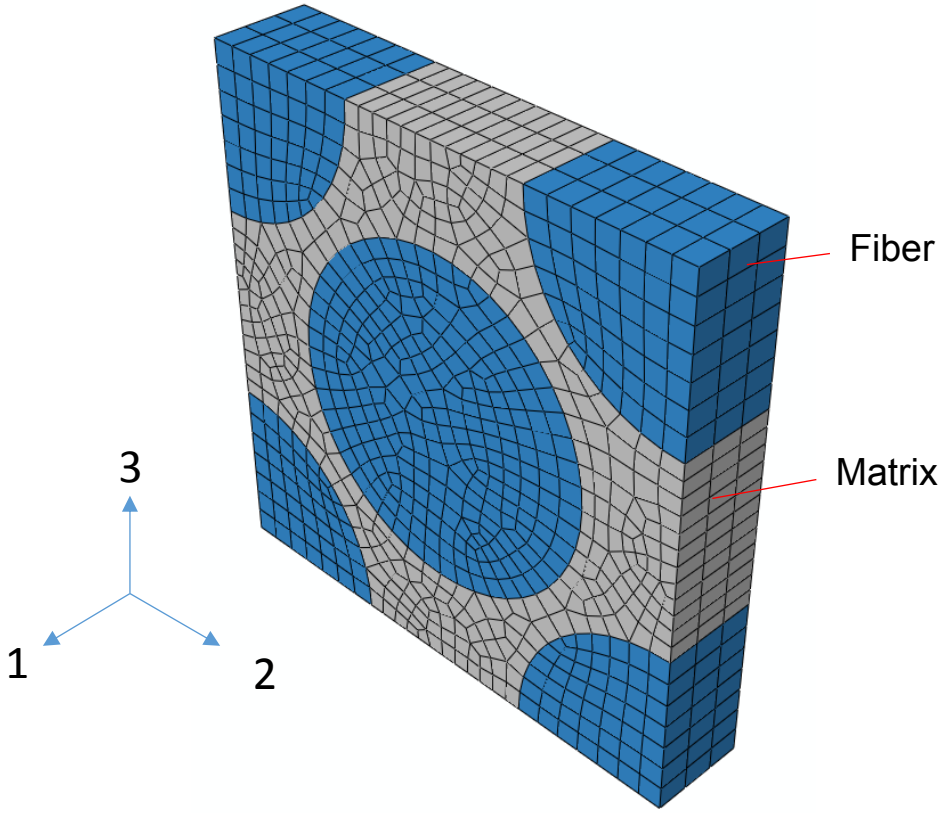

Figure 1. Representative volume element.

master curve is a universal function relating the effective stresses to the effective plastic strain for any loading conditions [15], including multiaxial loadings. In this study, the stress-strain curve for a normal loading in the 2-direction (see coordinate system in Fig. 1) is used to define the master curve, setting $a_{22}=1.0$ in Eqs. 15 and 16. As the master curve is determined, the values of a_{11}, a_{33}, a_{44}, a_{55}, and a_{66} can be specified by trial and error optimization to bring other curves into coincidence with the master $\bar{\sigma}$ *vs* $\bar{\varepsilon}^p$ curve. Note that the values of a_{11}, a_{22}, and a_{33} can also be obtained by using Eq. 6. Readers interested in the details of how to obtain these plasticity parameters are referred to Refs. 2 and 3.

Once the master $\bar{\sigma}$ *vs* $\bar{\varepsilon}^p$ curve is established, Eq. 10 can be used to write the scalar plastic multiplier $d\lambda$ as

$$d\lambda = \frac{3}{4}\frac{d\bar{\sigma}}{H_p\bar{\sigma}} \tag{19}$$

where $H_p = d\bar{\sigma}/d\bar{\varepsilon}^p$ is the slope of the master curve.

In the classical theory of plasticity [15-16], the incremental total strain is decomposed into the elastic part $\{d\varepsilon^e\}$ and plastic part $\{d\varepsilon^p\}$ as

$$\{d\varepsilon\} = \{d\varepsilon^e\} + \{d\varepsilon^p\}. \tag{20}$$

The explicit forms of $\{d\varepsilon\}$, $\{d\varepsilon^e\}$ and $\{d\varepsilon^p\}$ are

$$\begin{aligned}\{d\varepsilon\}^T &= \{d\varepsilon_{11}, d\varepsilon_{22}, d\varepsilon_{33}, d\gamma_{23}, d\gamma_{31}, d\gamma_{12}\}^T, \\ \{d\varepsilon^e\}^T &= \{d\varepsilon^e_{11}, d\varepsilon^e_{22}, d\varepsilon^e_{33}, d\gamma^e_{23}, d\gamma^e_{31}, d\gamma^e_{12}\}^T, \quad \text{and} \\ \{d\varepsilon^p\}^T &= \{d\varepsilon^p_{11}, d\varepsilon^p_{22}, d\varepsilon^p_{33}, d\gamma^p_{23}, d\gamma^p_{31}, d\gamma^p_{12}\}^T.\end{aligned} \tag{21}$$

The superscript *T* denotes a vector transpose. The elastic strain increments are defined as

$$\{d\varepsilon^e\} = [S^e]\{d\sigma\} \tag{22}$$

where $[S^e]$ is the elastic compliance matrix [21], and $\{d\sigma\}$ is the incremental stress vector. The plastic strain increments are defined as

$$\{d\varepsilon^p\} = [S^p]\{d\sigma\} \tag{23}$$

where $[S^p]$ is the plastic compliance matrix which can be expressed as [3]

$$S^p_{ij} = \mu C_i C_j \ , \quad i, j = 1, 2, ..., 6 \tag{24}$$

where $C_i = \frac{1}{2}\frac{\partial f}{\partial \sigma_i}$ and $\mu = \frac{9}{4}\frac{1}{\bar{\sigma}^2}\frac{1}{H_p}$.

Note that in the expression for C_i, the subscript i is defined as : 1=11, 2=22, 3=33, 4=23, 5=31, and 6=12. The elasto-plastic stress-strain equation, which relates the stress increments to the total strain, is

$$\{d\sigma\} = [D^{ep}]\{d\varepsilon\} \tag{25}$$

where the elastic-plastic stiffness matrix $[D^{ep}]$ is

$$[D^{ep}] = ([S^e] + [S^p])^{-1}. \tag{26}$$

A substepping scheme which is used to integrate Eq. 25 will be presented in detail later.

Micromechanics Model

In this study, a virtual testing approach is used to obtain the stress-strain curves for a unidirectional graphite/epoxy laminate by analyzing a RVE subjected to axial

(normal) and shear loadings, using Abaqus/Standard [22]. This RVE is a micromechanics model that has fiber and matrix modeled explicitly to represent the correct geometries, distinct material properties, and correct fiber volume fraction. The RVE model is shown in Fig. 1. Its dimensions are 0.001524 mm in the 1-direction, and 0.008207 mm in both 2- and 3- directions, and the fiber volume fraction is 62%. Periodic boundary conditions, which were found to be appropriate by Sun and Vaidya [20], are used for all the RVE analyses. The material modeled in this study is graphite/epoxy IM7/977-3. The fiber is modeled as a linear-elastic material and its properties [12] are listed in Table 1. The matrix is modeled with J2-plasticity and the effective-stress versus effective-plastic-strain curve of the matrix, shown in Fig. 2, is obtained from Ref. 12. The loading conditions applied include normal tensile loads in the 1- and 2- directions, transverse shear load, and longitudinal shear load. The loading directions and the appropriate boundary conditions for each loading case can be found in Ref. 20. The average (homogenized) stress and strain of the RVE may be obtained from

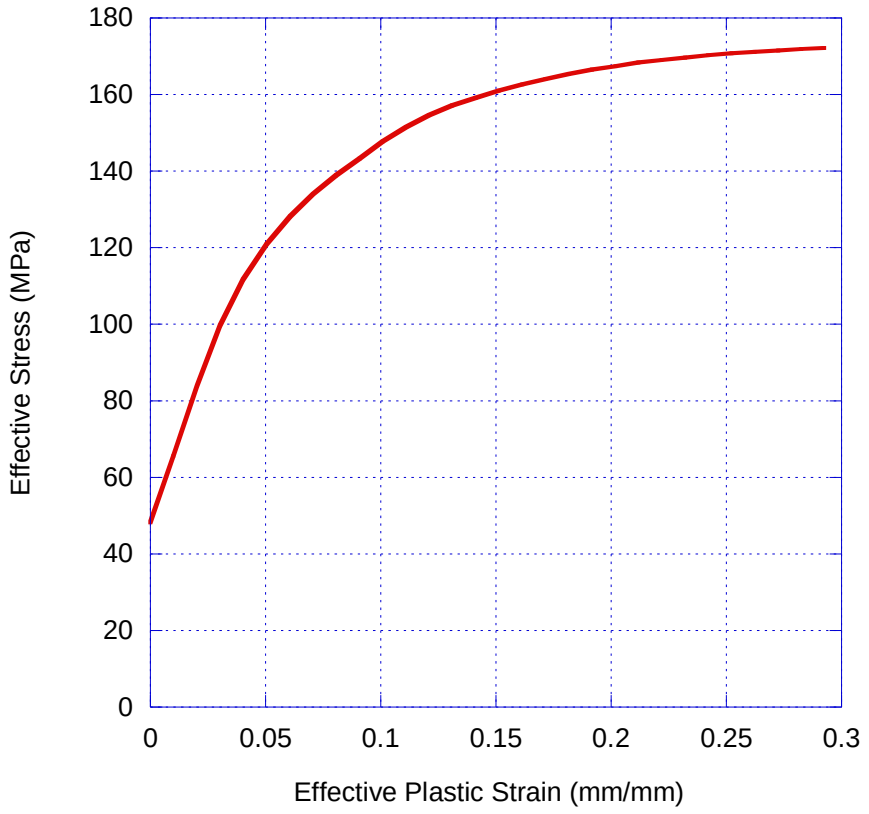

Figure 2. Effective stress and effective plastic strain of matrix obtained from Ref. 12.

$$\bar{\sigma}_{ij} = \frac{1}{V}\int_V \sigma_{ij}(x,y,z)dV \tag{27}$$

and

$$\bar{\varepsilon}_{ij} = \frac{1}{V}\int_V \varepsilon_{ij}(x,y,z)dV. \tag{28}$$

Alternatively, the average stress can be computed from the reaction forces, and the average strain can be computed from the surface displacements of the RVE by using Gauss's theorem. Abaqus [22] analyses were performed to obtain the reaction forces and surface displacements for each loading case. The average stress and average strain curves are used to establish the plasticity yield function. These averaged stress-strain curves are plotted in Figs. 3-6. Fig. 3 is the curve for tensile loading in the 1-direction (σ_1 *vs* ε_1); Fig. 4 is the curve for tensile loading in the 2-direction (σ_2 *vs* ε_2); Fig. 5 is the curve for the transverse shear loading (τ_{23} *vs* ε_{23}); and Fig. 6 is the curve for the shear loading in the 1-2 plane (τ_{12} *vs* ε_{12}). Note that ε_{22} and ε_{33} are also plotted in Figs. 3 and 4, so their plastic strains can be evaluated for computing PPRs (see Eq. 5). It is assumed the σ_3 *vs* ε_3 curve is the same as the σ_2 *vs* ε_2 curve and the τ_{13} *vs* ε_{13} curve is the same as the τ_{12} *vs* ε_{12} curve, due to transverse isotropy. Table 2 shows that the elastic moduli predicted by the micromechanics analysis (MMA) have good agreement with published data [23].

TABLE 1. IM7 FIBER PROPERTIES [12]

$E_1(GPa)$	256
$E_2, E_3(GPa)$	16
$G_{12}, G_{13}(GPa)$	15
$G_{23}(GPa)$	6.3
ν_{12}, ν_{13}	0.31
ν_{23}	0.28

TABLE 2. IM7/977-3 UNIDIRECTIONAL LAMINATE MATERIAL PROPERTIES

	Test [23]	Micromechanics Analysis Prediction
$E_1(GPa)$	164	160
$E_2, E_3(GPa)$	8.98	9.44
$G_{12}, G_{13}(GPa)$	5.02	4.15
$G_{23}(GPa)$	3.0	3.69
ν_{12}, ν_{13}	0.32	0.34
ν_{23}	0.496	0.5

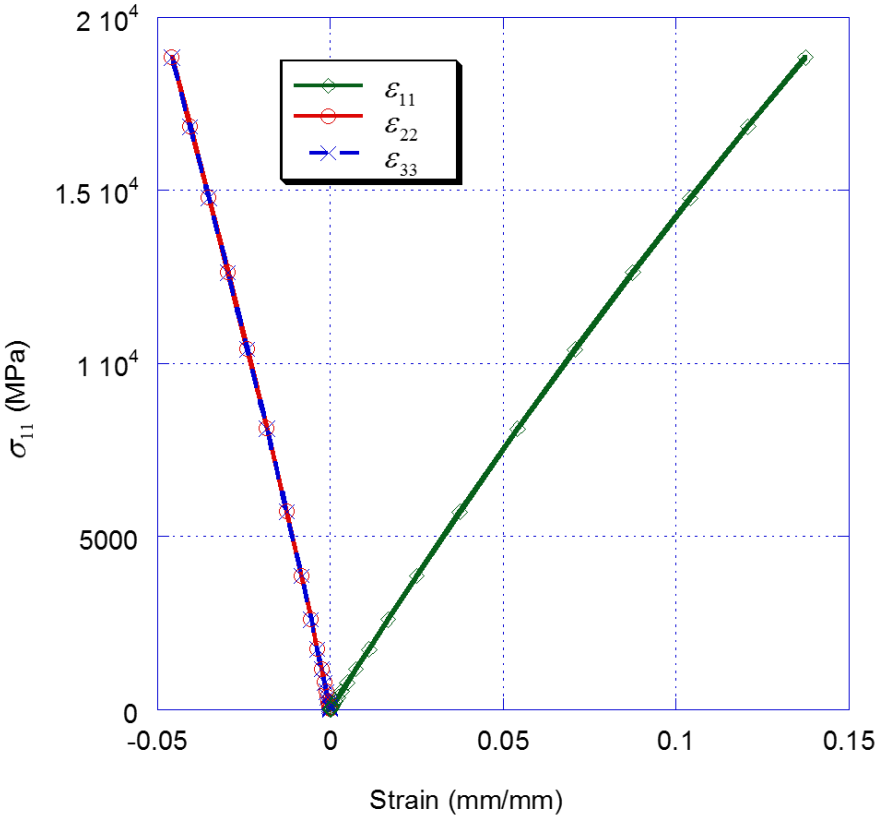

Figure 3. Stress-strain curve for tensile loading in fiber direction.

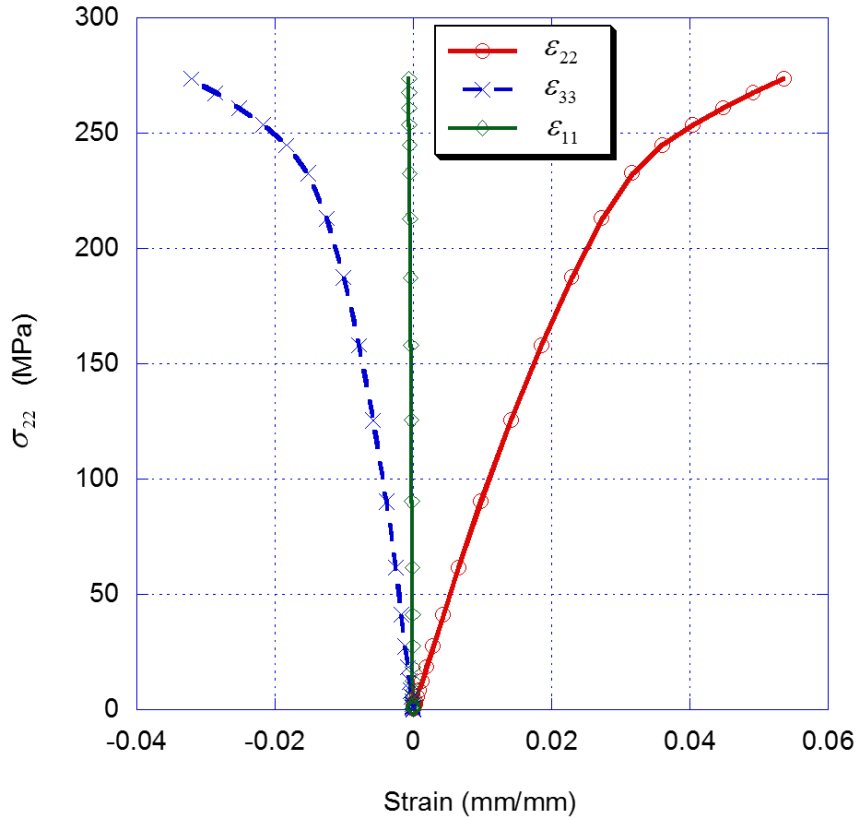

Figure 4. Stress-strain curve for tensile loading in transverse direction (2-direction).

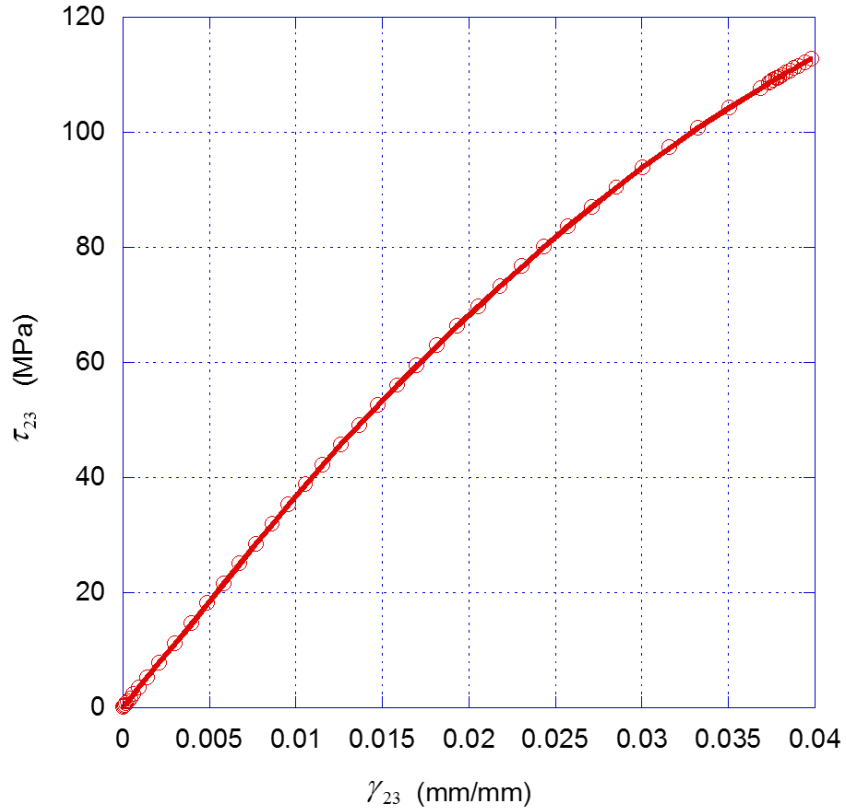

Figure 5. Stress-strain curve for transverse shear loading.

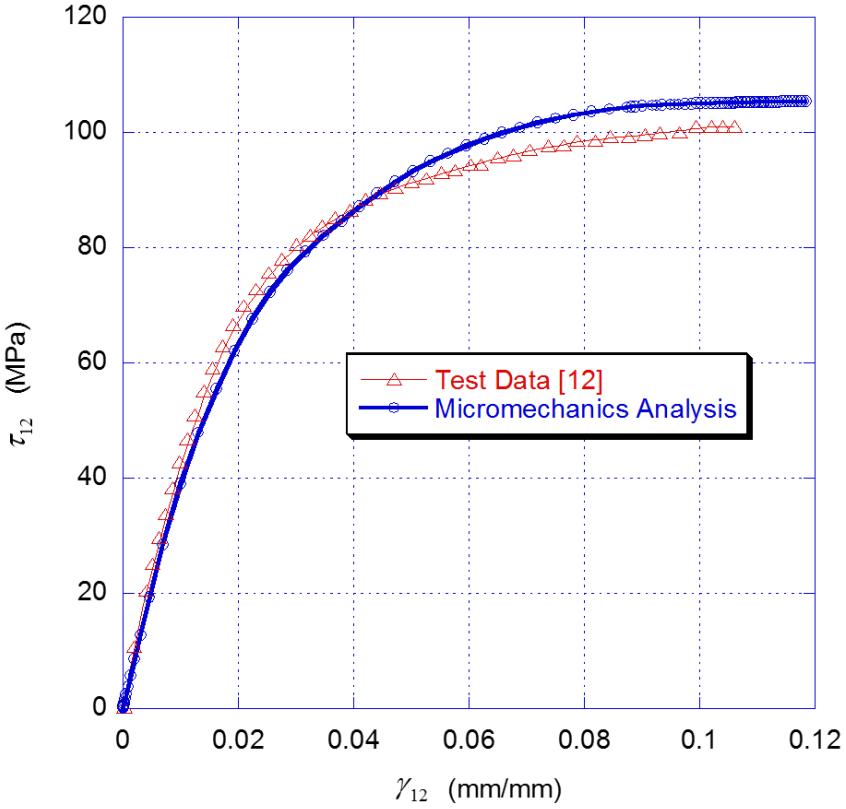

Figure 6. Stress-strain curve for shear loading in the 1-2 plane.

Determination of Plasticity Parameters

The values of the nine plasticity parameters in Eq. 1 can be determined through optimization [2]. They can also be defined by using the PPRs defined in Eq. 5. The plastic strains used for computing the PPRs can be determined from the stress-strain curves obtained by the uniaxial tension analyses of the RVE model [3]. Once the PPRs are determined, the plasticity parameters (a_{11}, a_{33}, a_{12}, a_{23}, and a_{13}) can be obtained by Eq. 6. Since transverse isotropy is assumed, this results in $\nu_{12}^p = \nu_{13}^p$, $\nu_{23}^p = \nu_{32}^p$, and $\nu_{21}^p = \nu_{31}^p$. The values of a_{44}, a_{55}, and a_{66} can be determined using the master $\bar{\sigma}$ *vs* $\bar{\varepsilon}^p$ curve. The procedures used by Ref. 3 are adopted for obtaining the plasticity parameters in this study. The determined plasticity parameters are given as follows:

$$\begin{aligned} &a_{11} = 0.000256, \quad a_{22} = a_{33} = 1.0, \\ &a_{23} = -0.8963, \quad a_{12} = a_{13} = -0.0006, \\ &a_{44} = 0.8, \qquad a_{55} = a_{66} = 3.4. \end{aligned} \tag{29}$$

It can be proven that the yield function with the above plastic parameters is always non-negative and the shape of the yield surface remains the same in hardening [3]. Using these plasticity parameters with Eqs. 15 to 18, all normal and shear stress-strain curves can be collapsed onto the master curve, as shown in Fig. 7.

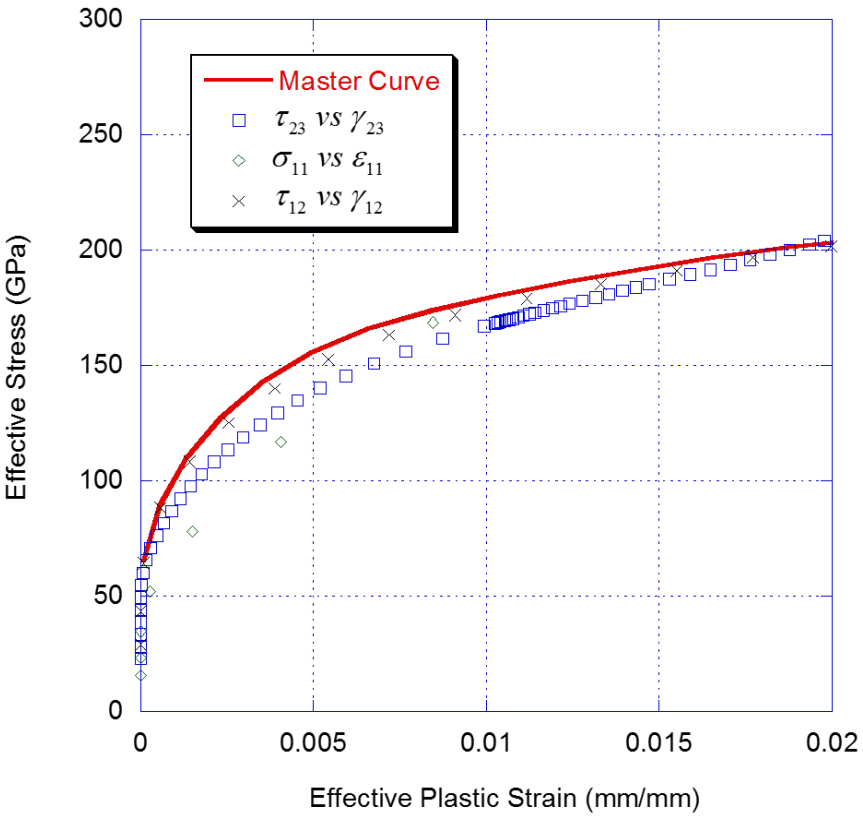

Figure 7. Master effective stress-effective plastic strain curve.

Integration of Elasto-plastic Stress-strain Relations

The substepping scheme developed by Sloan [19] is implemented in this study for numerical integration of the incremental elasto-plastic stress-strain relations, Eq. 25. This scheme was originally developed to work with the displacement controlled finite element method for analyzing elasto-plastic solids. Using displacement controlled loading, the stresses and strains are computed at element integration points for each stage of the solution. If the stresses at an integration point cause plastic yielding, the elastoplastic stress-strain relations, Eq. 25, are solved. The first-order Euler scheme is often used in finite element codes (see Refs. 17 and 18). Since the Euler scheme is accurate only for very small time steps, the finite element analysis time step, Δt, must be divided into smaller substeps. Traditionally, the number of substeps is determined from an empirical rule and all substeps are assumed to have the same size. This approach may result in computed stresses that do not satisfy the yield function at the end of each analysis time step, Δt, and the stresses must be restored to the yield surface. In this paper, the modified Euler scheme implemented by Sloan is used for solving incremental stresses for known incremental strains. This scheme does not require stress correction, and also has the ability to control the error in the integration of the elasto-plastic equations.

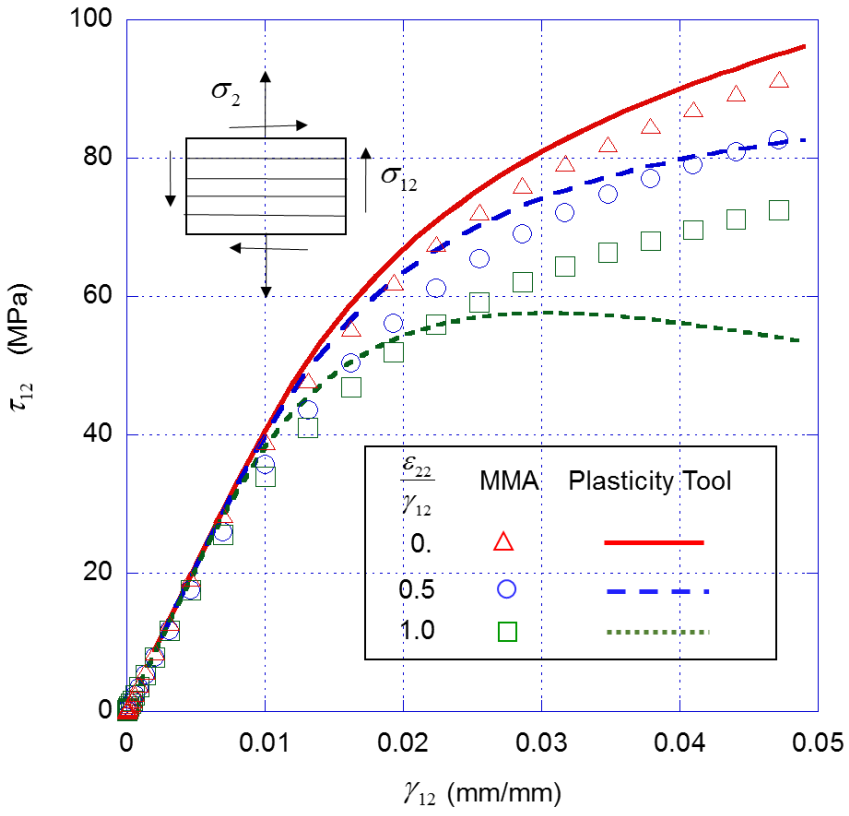

Figure 8. Stress-strain curves for unidirectional laminate subjected to transverse load and in-plane shear, increase of transverse tension stress reducing shear stress is predicted by both MMA and the plasticity tool.

INTERACTION OF MULTIAXIAL STRESSES

The plasticity tool implemented in this study is used to predict the nonlinear shear behavior of a unidirectional laminate subjected to multiaxial loadings. The problem solved is similar to the study on the effect of transverse stress on shear stress-strain behavior investigated by Huang and Liechti [4]. In this study, a unidirectional laminate, shown in Fig. 8, is subjected to multiaxial loading: transverse tensile load and in-plane shear loads. It is found, via integration of Eq. 25, that at a constant shear strain level, an increase in transverse tensile stress can reduce shear stress. This finding agrees with that presented in Ref 4. The effect of transverse tensile stress on the shear stress shown in Fig. 8 cannot be predicted with a linear elastic analysis.

The results obtained from MMA of the RVE with boundary conditions chosen to produce the same ratios of $\varepsilon_{22} / \gamma_{12}$ are also shown in Fig. 8. Note that the periodic boundary conditions of the RVE were not used here, since they allow deformations in all directions, which can result in a more flexible model than the one considered here. These MMA results reveal the same trend, at a constant shear strain level, namely an increase in transverse tensile stress, expressed as $\varepsilon_{22} / \gamma_{12}$, can reduce shear stress. The shear stresses predicted by the MMA have good agreement with the predictions of the plasticity tool. For the case of $\varepsilon_{22} / \gamma_{12} = 1$, the shear stresses are under-predicted by the plasticity tool at strain levels above 2.5%. However, at that high transverse strain level, discrete matrix cracks may have occurred. Since modeling failure is not in the scope of the current study, data for transverse strain levels above 2.5% shown in Fig. 8 may be invalid.

CONCLUDING REMARKS

This study implemented a plasticity tool to predict the nonlinear shear behavior of unidirectional composite laminates with an intent to further develop the tool for use in composite PDA. The steps for developing the plasticity tool include establishing a yield function, deriving the incremental elasto-plastic stress-strain relations using the yield function with an associated flow rule, and integrating the elasto-plastic stress-strain relations to predict the shear nonlinearity of unidirectional laminates under multiaxial loads. A substepping scheme was used to integrate the elasto-plastic stress-strain relations. This scheme is suitable for displacement-based finite element codes; thus it can be incorporated with commercial finite element codes for laminated composite analyses.

In this study, micromechanics analyses were performed to obtain normal and shear stress-strain curves for determining the plasticity parameters of the yield function. This virtual testing approach can be used to replace the costly experimental tests for obtaining stress-strain responses of composites under various loading conditions. The predicted elastic moduli and Poisson's ratios are in good agreement with experimental data.

The plasticity tool implemented in this study was used to predict the nonlinear shear behavior of a unidirectional laminate subjected to multiaxial loadings. A unidirectional laminate was subjected to transverse load and in-plane shear loadings. It was found that at a constant shear strain level, increasing transverse tensile stress

can reduce the shear stress. This transverse tensile stress effect on the shear stress, which agrees with published findings [4], cannot be predicted with linear elastic analysis.

REFERENCES

1. Sun, C.T. and J.L. Chen. 1989. "A Simple Flow Rule for Characterizing Nonlinear Behavior of Fiber Composites," *J. Composite Materials*, 23:1009-1020.
2. Xie, M. and D.F. Adams. 1995. "A Plasticity Model for Unidirectional Composite Materials and its Applications in Modeling Composite Testing," *Composites Science and Technology*, 54:11-21.
3. Chen, J.K., F.A. Allahdadi and C.T. Sun. 1997. "A Quadratic Yield Function for Fiber-Reinforced Composites," *Journal of Composite Materi*als, 31(8):788-811.
4. Hung, S.-C., and K.M. Liechti. 2000. "Nonlinear Multiaxial Behavior and Failure of Fiber-Reinforced Composites," *Time Dependent and Nonlinear Effects in Polymers and Composites, ASTM STP 1357*, R. A. Schapery and C. T. Sun, Eds., American Society for Testing and Materials, West Conshohocken, PA, 176-222.
5. Goldberg, R.K., K.S. Carney, P. Dubois, C. Hoffarth, J. Harrington, S. Rajan and G. Blankenhorn. 2014. *Theoretical Development of an Orthotropic Elasto-Plastic Generalized Composite Material Model*, NASA/TM-2014-218347.
6. Goldberg, R.K., K.S. Carney, P. Dubois, C. Hoffarth, J. Harrington, S. Rajan and G. Blankenhorn. 2016. *Analysis and Characterization of Damage Utilizing an Orthotropic Generalized Composite Material Model Suitable for Use in Impact Problems*, NASA/TM-2016-218959.
7. Wang, S.S., S. Srinivasan, H.T. Hu, and R.M. Haj-Ali. 1995. "Effect of Material Nonlinearity on Buckling and Postbuckling of Fiber Composite Laminated Plates and Cylindrical Shells," *Composite Structures*, 33:7-15.
8. Schapery, R.A. 1989. *Mechanical Characterization and Analysis of Inelastic Composite Laminates with Growing Damage*, Mechanics & Materials Center Report 5762-89-10, Texas A & M University, College Station, TX.
9. Schapery, R.A. 1990. "A Theory of Mechanical Behavior of Elastic Media with Growing Damage and Other Changes in Structure," *J. Mech. Phys. Solids*, 38(2):1725–1797.
10. Sicking, D.L. 1992. *Mechanical Characterization of Nonlinear Laminated Composites with Transverse Crack Growth*, Ph.D. thesis, Texas A&M University, College Station, TX.
11. Pineda, E.J. and A.M. Waas. 2013. "Numerical Implementation of a Multiple-ISV Thermodynamically-Based Work Potential Theory for Modeling Progressive Damage and Failure in Fiber-Reinforced Laminates," *Int. J. Fracture*, 182(1):93-122.
12. Stier B., P. Naghipour, E.J. Pineda, L. Hanson, S.M. Arnold, B.A. Bednarcyk, and A.M. Waas. 2015. "Multiscale Static Analysis of Notched and Un-notched Laminates Using the Generalized Method of Cells," AIAA-2015-1881, AIAA SciTech, 56th AIAA/ASCE/AHS/ASC Structures, Structural Dynamics, and Materials Conference, 5-9 January 2015, Kissimmee, Florida.
13. Zhang, D. and A.M. Waas. 2014. "A Micromechanics Based Multiscale Model for Nonlinear Composites," *Acta Mech*., 225:1391-1417.
14. Hill, R. 1950. *Mathematical Theory of Plasticity*, Oxford University Press, London.
15. Khan, A.S. and S. Huang. 1995. *Continuum Theory of Plasticity*, John Wiley and Sons, New York.
16. Lubliner, J. 2008. *Plasticity Theory*, Dover Publications, Inc., Mineola, NY.
17. Nayak, G.C. and O.C. Zienkiewicz. 1972. "Elasto-Plastic Stress Analysis: A Generalization for Various Constitutive Laws Including Strain Softening," *International Journal for Numerical Methods in Engineering*, 5:113-135.
18. Owen, D.R.J. and E. Hinton. 1980. *Finite Elements in Plasticity: Theory and Practice*, Pineridge Press, West Cross Lane, Swansea, U.K.
19. Sloan, S.W. 1987. "Substepping Schemes for the Numerical Integration of Elasto-plastic Stress-Strain Relations," *Int. J. Numer. Meth. Eng.*, 24:893-911.
20. Sun, C.T. and R.S. Vaidya. 1996. "Prediction of Composite Properties from a Representative Volume Element," *Composites Science and Technology*, 56:171-179.

21. Jones, R.M. 1999. *Mechanics of Composite Materials*, Second edition, Taylor & Francis, Inc., Philadelphia, PA.
22. Abaqus. 2013. Abaqus Analysis User's Guide (Abaqus Online Documentation), Version 6.13. Dassault Systems Simulia Corp., Providence, RI.
23. Clay, S. and R. Holzwarth. 2014. "Quantitative Assessment of Progressive Damage Tools for Composites," Proceedings of the American Society for Composites 2014-Twenty-nineth Technical Conference on Composite Materials, University of California San Diego, La Jolla, CA.